# Strain measurement range enhanced chirped pulse φ-OTDR for distributed static and dynamic strain measurement based on random fiber grating array

Wang, Yuan; Lu, Ping; Mihailov, Stephen; Chen, Liang; Bao, Xiaoyi



**Publisher's version / Version de l'éditeur:**
https://doi.org/10.1364/OL.405768
*Optics Letters, 45, 21, pp. 6110-6113, 2020-11-01*

Optics Letters

# Strain measurement range enhanced chirped pulse $\varphi$-OTDR for distributed static and dynamic strain measurement based on random fiber grating array

Yuan Wang,[1] Ping Lu,[2] Stephen Mihailov,[2] Liang Chen,[3] and Xiaoyi Bao[1,3,*]

[1]School of Electrical Engineering and Computer Science, University of Ottawa, Ottawa, Ontario K1N 6N5, Canada
[2]National Research Council Canada, Ottawa, Ontario K1A 0R6, Canada
[3]Department of Physics, University of Ottawa, 25 Templeton Street, Ottawa, Ontario K1N 6N5, Canada
*Corresponding author: xbao@uottawa.ca

Received 18 August 2020; revised 2 October 2020; accepted 5 October 2020; posted 5 October 2020 (Doc. ID 405768); published 1 November 2020

**A high-performance distributed sensing system based on a random fiber grating array (RFGA) and multi-frequency database demodulation (MFDD) method for strain induced delay time measurement is demonstrated. It enables a wide measurement range for both static and dynamic strain sensing. The proposed MFDD method can enlarge the strain measurement range, since the large strain variation induced time domain trace distortion could be compensated for by laser initial frequency changes. Furthermore, a random fiber grating made with embedded large random refractive index changes along the single-mode fiber could provide a stable reflection with a wide reflection spectrum range. Such a structure successfully improves the time delay measurement precision and achieves a large tuning range, as demonstrated by the database in which a set of pre-recorded undisturbed reflected Rayleigh traces form RFGA at various laser frequencies. Ultimately, a dynamic strain with a peak-to-peak value of 12.5 με at a vibration frequency of 50 Hz is accurately reconstructed when the pulse repetition rate is 1 kHz, which was not detected using a conventional chirped pulse phase-sensitive optical frequency domain reflectometers. The maximum measurable strain variation of about 12.5 με represents a factor of 3 improvement. This number is limited by a pre-recorded frequency scanning range of RFGA response in the database.** 

https://doi.org/10.1364/OL.405768

Distributed optical fiber sensors (DOFSs) can detect strain or temperature variations along the entire fiber length, which plays an increasingly important role in fields of structural health monitoring and intruder detection. Various DOFSs have been researched and demonstrated for quantitative strain sensing, such as Brillouin optical time domain analysis (BOTDA), phase-sensitive optical frequency domain reflectometers ($\varphi$-OTDRs) and optical frequency domain reflectometers (OFDRs) [1–4]. The distributed strain measurement is achieved by measuring Brillouin frequency shift (BOTDA), phase shift ($\varphi$-OTDR) or wavelength shift (OFDR) at every position in the fiber. Among them, $\varphi$-OTDRs have higher strain sensitivity to reach n$\varepsilon$ levels based on phase demodulation by using ultra narrow line width lasers (3 kHz) [5]. However, the strain range is limited by the unwrapping algorithm used in $\varphi$-OTDR, since the demodulated phase is distorted when the absolute value of the phase jump between two consecutive points is larger than $\pi$. To solve the problem, a two-wavelength OTDR is proposed [6]. Such an approach makes the system complex and expensive due to the requirement for two phase-locked lasers. Besides, phase demodulation based on optical interferometry is sensitive to strain and temperature which imposed an environmental dependence. It is important to limit the usage of a phase demodulation based phase-locked laser and interferometry in order to reduce the overall system cost and environmental sensitivity.

Recently, a novel $\varphi$-OTDR sensing system using a distributed feedback (DFB) laser without an optical interferometer-based phase demodulation scheme is proposed [7]. Perturbation (strain or temperature variation) induced optical path length changes are translated into local time delays within the time window of optical trace. The principal advantage of this scheme is that real-time high-accuracy strain (nε) measurements are achieved by using a low-cost DFB laser (1 MHz), where no environmental dependence in demodulation process is observed. However, distortions in OTDR traces appear for large strain or temperature variations. This is due to the position dependence in time delay determination and introduces a large error for strain or temperature reconstruction. Therefore, the maximum measurable strain is limited to <1 με. In some particular applications, such as crack detection on civil structures or railway lines, large strain measurements ranges are required for the detection of arbitrarily large and unknown perturbations. In reference [8], dynamic strain variation of 1190 με at a vibrational frequency of 400 Hz has been successfully reconstructed when the high repetition rate of an interrogation system was used (200 kHz). However, the total sensing distance, which is related to the pulse repetition rate, will be significantly reduced. Another potential method to enhance the measurement range is to increase the chirping slope of the chirped pulse. However, this approach reduces the sensitivity of the system (minimum detectable strain variation). There is a trade-off between the strain resolution and the sensing range.

In this Letter, a novel approach based on the multi-frequency database demodulation (MFDD) method is proposed and demonstrated to improve the strain measurement range for both static and dynamic strain measurements. In order to improve the time delay measurement precision, a random fiber grating array (RFGA) with a larger index change range is utilized as a stable reflected trace provider [9]. The RFGA with a number of artificial refractive index planes enables a wide-wavelength reflection [10], which always offers reflection when the initial frequency of the DFB laser experiences, a large tuning range in the established database.

Chirped pulse phase OTDR (CP $\varphi$-OTDR), which makes use of the Rayleigh backward scattering effect, has been widely used for the measurement of perturbations along an optical fiber. The major difference when compared with traditional phase OTDR is that the optical frequency of integration pulses used here has a linear variation. The instantaneous optical frequency profile of the chirped pulse is then expressed as [7]

$$\upsilon(t) = \left(\upsilon_0 + \frac{\Delta\upsilon}{W}\cdot t\right)\mathrm{Rect}(t/W), \tag{1}$$

where Rect is the rectangular function, $\upsilon_0$ is the initial optical frequency of chirped pulse, and $W$ and $\Delta\upsilon$ are the pulse width and the spectral content of the chirped pulse, respectively. If this chirped pulse is sent to a section of optical fiber, the optical power at the input end of the optical fiber at given time $t$ is expressed as

$$I(t)_{AC} = I_0 \int_{(t-W)c/2n}^{tc/2n}\int_{(t-W)c/2n}^{tc/2n} e^{-2\alpha(Z_i+Z_j)} r(Z_i)\cdot r(Z_j) \cdot e^{i[\Delta\varphi_{ij}(t)]}\mathrm{d}z_i\mathrm{d}z_j, \tag{2}$$

where $n$ is the average value of refractive index, and $c$ is the velocity of light in a vacuum. $\alpha$ is the average attenuation of the unit–length random grating array; $Z_i$ and $Z_j$ are the fiber length between the input end of fiber and scattering center $i$th or $j$th; $I_0$ is input power of the light; and $r(Z_i)$ and $r(Z_j)$ are the reflection coefficient of scattering center $i$th and $j$th, respectively. $\Delta\varphi_{ij}(t)$ is the phase difference between two scattering center $i$th and $j$th, which could be expressed as [7]

$$\Delta\varphi_{ij}(t) = 2\pi\int_{t-2nZ_j/c}^{t-2nZ_i/c}(\upsilon_0 + \Delta\upsilon\cdot t/W)\mathrm{d}t = 2\pi\left[\left(\frac{2n(Z_i-Z_j)}{c}\right)\left(\upsilon_0 + \frac{\Delta\upsilon}{W}(t - \frac{n(Z_i+Z_j)}{c}\right)\right]. \tag{3}$$

From Eqs. (2) and (3), we find that the shape of reflected trace from optical fiber is associated with the phase of the reflected electrical field, which is determined by the optical frequency of the laser source and the optical path length between any two scattering centers. Therefore, if a strain or temperature induced variation in the trace shape occurs at one position, the specific time delay between two given times $t_0$ and $t_1$ from two time domain traces (before and after strain is applied) that could be used to compensate for the strain induced traces distortion [7]. On the other hand, a corresponding optical frequency shift of the laser source also can be applied to reconstruct the changed trace to the previous state [2]. Therefore, the applied strain variation $\Delta\varepsilon$ can be extracted based on both the time delay $\Delta t$ and the initial frequency difference of chirped pulse $\upsilon_1 - \upsilon_0$ such that

$$\Delta\varepsilon\cdot K = \frac{\Delta nl + n\Delta l}{nl} = -\frac{\frac{\Delta\upsilon}{W}\Delta t + (\upsilon_1 - \upsilon_0)}{\upsilon_0}, \tag{4}$$

where $K$ is a strain related frequency shift coefficient (equals to $-0.59$ in RFGA) [7,11]. $\upsilon_1$ is the initial frequency of the reference trace in the database which has highest similarity with the encoded trace.

Based on the discussion above, we find that the maximum measurable strain variation $\Delta\varepsilon$ is significantly improved if we use a database composed of various traces which are collected from chirped pulses with different initial optical frequencies. The MFDD method is proposed and operated as follows: first, a database including several traces without perturbation is established. These traces are collected when chirped pulses with different initial optical frequencies [$\upsilon_0$ in Eq. (1)] are used to interrogate the whole RFGA. Secondly, coded traces are recorded using chirped pulses with known fixed initial optical frequencies when dynamic strain is applied in a period of time. Thirdly, in the demodulation process, the cross-correlation calculation between each encoded trace and each reference trace in the database is employed. Finally, the cross-correlation calculation result of each coded trace which possesses the highest coefficient will be selected for relative strain change determination. The overall strain variation is reconstructed based on the initial frequency difference $\upsilon_1 - \upsilon_0$ and time delay $\Delta t$ without integral operation.

The setup of our proposed system is shown in Fig. 1. A DFB laser diode (CQF938/500, JDS Uniphase) driven by an adjustable DC current source is utilized to generate chirped pulses. The chirped pulse is produced by a pulse generator (PG) (8130A, Hewlett Packard) combined with a semiconductor optical amplifier (SOA) (OPB-10-10-N-C-FA, Kamelian) synchronized through the PG. The pulse generator (PG) introduces a frequency sweep of output light by adding an electrical modulation pulse signal with 10 ns rising edge and 10 ns falling edge to the DFB laser. The output light of the DFB laser is changed into a chirped pulse signal by the SOA that is driven by a homemade electronic circuit board. The chirped pulse signal with 6 ns pulse width and a 1.375 GHz frequency content is amplified by an erbium-doped fiber amplifier (EDFA) before being sent to the strong RFGA. The one end of the RFGA is fixed on a translation stage, while the other end is glued to the top of a piezoelectric transducer (PZT) device (P-6113S, PI). The displacement of the PZT device can be precisely controlled by an electrical signal. The backward scattered signal from the strong RFGA is detected by a 40 G bandwidth photodetector (DSCH10H-39-FC, Discovery Semiconductor Inc.). An optical filter (OSP-9100, Newport) is used to remove the ASE noise from the EDFA. Ultimately, the time domain traces are collected by an oscilloscope (OSC) (DSO81204B, Agilent). For optical

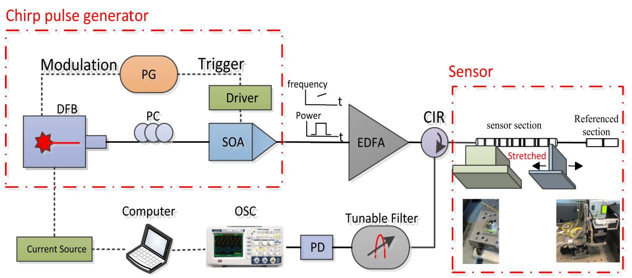


**Fig. 1.** Experimental setup of an RFGA-based distributed sensor for static and dynamic strain sensing.

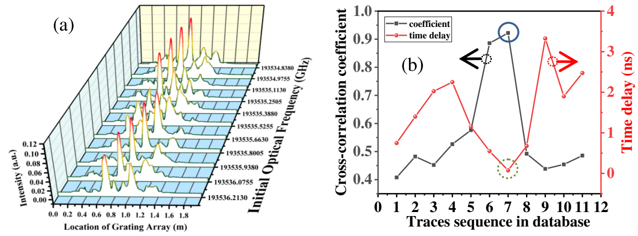


**Fig. 3.** (a) 11 reflected traces of RFGA in a database when different initial optical frequencies of chirped pulses are used; (b) 11 cross-correlation results between encoded traces and traces in a database.

frequency sweeping purposes, the computer is employed to change the output of the current source and synchronize the OSC for trace collection.

A crucial factor of the feasibility of the proposed method is the issue of larger time delay measurement uncertainty [11]. In our proposed system, the refractive index changes of the strong RFGA were fabricated along the single-mode fiber (SMF) by the fiber to a femtosecond (fs)-IR pulsed laser through the plane-by-plane technique [12]. The RFGA was 0.8 m in length including 8 alternating sub-gratings that are 10 mm and 5 mm long, respectively. The grating periods of all 8 sub-gratings are randomly distributed between 0.5180 and 0.5464 μm [7]. Because of its larger index change range ($10^{-5}$) as compared to scattering levels from the SMF, the RFGA reflection could reach −30 dB (SMF is about −70 dB); thus, the (signal-to-noise ratio) SNR of the trace could be enhanced. More importantly, the crosstalk effect induced distortion is negligible when refection of a sensor is around −30 dB.

A time delay measurement precision evaluation was carried out first. As shown in Fig. 2(a), 1000 traces were collected by OSC using a chirped pulse with a fixed initial optical frequency when no perturbation was applied. The pulse repetition rate was 1 kHz, and the total acquisition time was 1 s. In order to distinguish the tiny temporal shift of 1000 traces, a cross-correlation calculation between the current and subsequent traces is performed (trace No. 1 with trace No. 2, trace No. 2 with trace No. 3, and …). The result, as shown in the inset figure of Fig. 2(a), indicates the high SNR of the reflected traces from RFGA over the acquisition time. Figure 2(b) depicts the histogram of the temporal shift fluctuations of the reflected traces with a standard deviation of about 31.8 ps, which indicates that the low SNR induced temporal shift noise is effectively suppressed, and the laser frequency drifting could be ignored within 1 s.

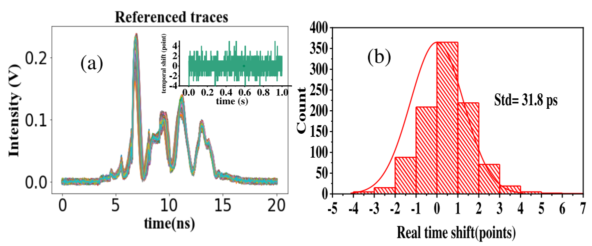


**Fig. 2.** Evaluation of the time delay measurement in CP $\varphi$-OTDR based on RFGA. (a) 1000 traces (no average) and (b) the temporal shift standard deviation. (The inset figure shows the temporal shift of traces over an acquisition time of 1 s.)

Before applying the strain, the database should be established for demodulation under the condition of no applied strain. The current source is precisely controlled by software, and the tuning step is 1 mA (±0.01 mA). As shown in Fig. 3, the 11 collected traces that represent the impulse response from the RFGA are collected when the initial optical frequency of chirped pulses is adjusted from 193536.213 (±0.005) GHz to 193534.838 (±0.005) GHz with tuning step of 0.1375 GHz. One encoded trace collected under a certain value of strain is used to calculate the cross correlation with 11 referenced traces in the database, as shown in Fig. 3(b). There are 11 pairs of time delay values and coefficient values after the cross-correlation calculation. It is obvious that the highest coefficient should be selected for the strain variation calculation, since higher coefficients represent a higher similarity between the two traces and thus a higher time delay estimation accuracy. In Fig. 3(b), the result of the trace sequence of 7 has the highest coefficient (blue solid circle), so its corresponding time delays (green dashed circle) will be selected for strain variation determination. At every measurement, the coefficient will be re-selected, and the highest one will be picked.

In order to compare the system performance with and without the MFDD method, static and dynamic strain measurements were performed. In our experiment, the strain was applied on the sensor section (as shown in Fig. 3) through the translation stage and high-precision PZT. For static measurements, different strain variations were applied to the RFGA, and its corresponding reflected traces were collected. As shown in Eq. (4), the applied strain induced optical path length change is translated into a local time delay within the time window. Thus, the cross-correlation calculation between the two traces is a valid method to extract local time delay information. In the demodulation process, the cross-correlation calculation is performed between the two traces obtained before and after applying the strain variation without using a database. Figure 4(c) illustrates the cross-correlation coefficient variation when different stains are applied. It is obvious that the cross-correlation coefficient decreases significantly with increasing levels of applied strain, as shown by the appearance of the distortions of the OTDR traces in Fig. 4(b). Therefore, the similarity of the two traces will obviously decrease, which is embodied through the low cross-correlation coefficient. However, the cross-correlation coefficient maintains a high value under large strain variation when the database is used, since the large strain variation induced optical path length change is compensated for by both the initial optical frequency difference and the time delay [Eq. (4)]. As depicted in Fig. 4(a), the larger strain variation also gives a high coefficient value when the database is utilized,

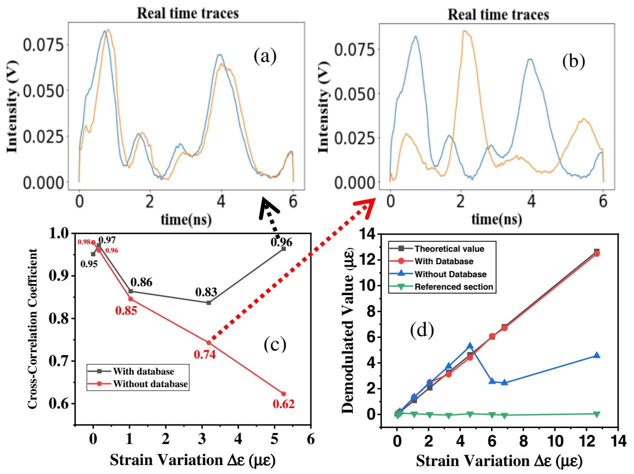


**Fig. 4.** (a) Reflected trace after applying strain on the RFGA and most similar trace in a database. (b) Reflected traces before and after applying strain on the RFGA. (c) Relationship between the cross-correlation coefficient and different applied strains. (d) Performance of demodulation with and without a database.

since the initial optical frequency difference compensates for a part of the strain variation, resulting in a small time delay. The applied strain variation and its demodulation resulting from the different methods are shown in Fig. 4(d). The figure clearly shows that the maximum measurable strain variation is significantly enhanced by using the MFDD method. The demodulation result of the reference section (no strain applied) is also obtained at the same time, which proves the capacity for distributed sensing. In our experiment, the selected time window for cross-correlation calculation is 6 ns, as shown in Fig. 4(a), so the spatial resolution is about 1.2 m. The maximum measurable strain variation is about 4.5 με without the MFDD method. While the maximum measurable strain variation for the MFDD method is about 12.5 με with a standard deviation of 66 nε, the minimum detectable strain variation dependent on the time delay measurement precision is about 66 nε.

Figure 5 illustrates the result of a dynamic strain measurement in which a fixed peak-to-peak 12.5 με (10 μm length change) strain change and different vibration frequencies are applied on the RFGA. The repetition rate of the chirped pulse for all the measurements is fixed at 1 kHz. When the vibration frequency is low, for example 10 Hz, each vibration period has 50 sampling points. In this case, the dynamic strain variation is perfectly revealed by using both methods, as shown in Fig. 5(a). In Fig. 5(c), the frequency response of the demodulated dynamic strain variation indicates a dominant peak precisely locating at 10 Hz with a high SNR up to 43 dB. However, there is a big difference between the two methods when the frequency of applied strain variation is 50 Hz, as shown in Fig. 5(b). Because of fewer sampling points (10 samples) within the vibration period, the strain variation between some of the two sampling points is close to the maximum value. Thus, the cross-correlation coefficient between the two traces is very low according to Fig. 4(c). The demodulation results will suffer from a large uncertainty in the delay time estimation, which leads to an incorrect reconstructed wave. In comparison, the demodulation process with the MFDD method maintained a good result. In Fig. 5(d), the zero padding method is used for peak location determination. A dominant peak representing 50 Hz is shown in inset figure.

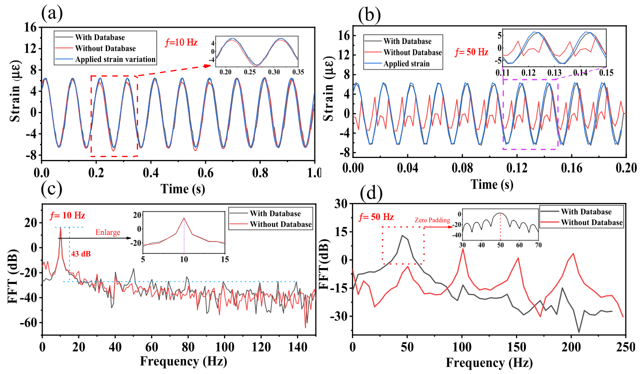


**Fig. 5.** Demodulated dynamic strains of two different methods (with and without a database); (a) 10 Hz sinusoidal variation and (b) 50 Hz sinusoidal variation and its frequency responses (c) and (d).

For dynamic strain measurement, the MFDD method significantly improves the maximum detectable vibration frequency. If the size of the database is large enough, the maximum detectable vibration frequency can reach the theoretical limit which is equal to half of the pulse repetition rate.

To summarize, a high-performance CP $\varphi$-OTDR based on both the MFDD method and an RFGA is proposed and demonstrated for both static and dynamic strain detection. The RGFA possesses a wide reflection spectrum range and variable width peaks in time domain, which achieves high time delay sensing accuracy. The experimental results show that the proposed MFDD method could effectively solve the measurement range limitation which is caused by a large time delay estimation error, indicating an attractive potential for this approach in the field of structural health monitoring.

**Funding.** China Scholarship Council (201808330421); Natural Sciences and Engineering Research Council of Canada (RGPIN-2015-06071, STPGP 506628); Canada Research Chairs (950231352).

**Disclosures.** The authors declare no conflicts of interest.

## REFERENCES


1. Y. Dong, D. Ba, T. Jiang, D. Zhou, H. Zhang, C. Zhu, Z. Lu, H. Li, L. Chen, and X. Bao, IEEE Photonics J. **5**, 2600407 (2013).
2. Y. Koyamada, M. Imahama, K. Kubota, and K. Hogari, J. Lightwave Technol. **27**, 1142 (2009).
3. S. Zhao, J. Cui, L. Suo, Z. Wu, D. Zhou, and J. Tan, J. Lightwave Technol. **37**, 3721 (2019).
4. A. Masoudi and T. Newson, Rev. Sci. Instrum. **87**, 011501 (2016).
5. Y. Dong, X. Chen, E. Liu, C. Fu, H. Zhang, and Z. Lu, Appl. Opt. **55**, 7810 (2016).
6. H. He, L. Yan, H. Qian, X. Zhang, B. Luo, and W. Pan, Opt. Express **28**, 226 (2020).
7. Y. Wang, P. Lu, S. Mihailov, L. Chen, and X. Bao, Opt. Lett. **45**, 3423 (2020).
8. H. D. Bhatta, L. Costa, A. Garcia-Ruiz, M. R. Fernandez-Ruiz, H. F. Martins, M. Tur, and M. Gonzalez-Herraez, J. Lightwave Technol. **37**, 4888 (2019).
9. Z. Zhou, P. Lu, L. Zhang, S. Mihailov, L. Chen, and X. Bao, Opt. Lett. **44**, 4195 (2019).
10. L. Zhang, P. Lu, Z. Zhou, Y. Wang, S. Mihailov, L. Chen, and X. Bao, IEEE Sens. J. **20**, 5885 (2020).
11. M. R. Fernandez-Ruiz, L. Costa, and H. F. Martins, Sensors **19**, 4368 (2019).
12. P. Lu, S. Mihailov, D. Coulas, H. Ding, and X. Bao, J. Lightwave Technol. **37**, 4697 (2019).